CHAPTER IV
RESULTS AND DISCUSSION

4.1 Characterization of Chitosan Starting Material

The starting material, chitosan, showed the intrinsic viscosity 346. The molecular weight of commercial chitosan is usually in the range of 10^5 and the viscosity reaches or exceeds 1 500 cps (Sugano *et al.*, 1992). Thus, it was concerned to be low viscosity chitosan. The solubility in acetic acid was found to be as high as 5% chitosan concentration in 10% acetic acid aqueous solution.

4.1.1 Chemical Structure Analysis of Chitosan

FT-IR spectrum of the chitosan with a degree of deacetylation 75.8% is shown in Figure 4.1.

The elemental analysis (EA) of chitosan DD 75.8%; $(C_6H_{11}NO_4)_{0.758}$ $(C_8H_{13}NO_5)_{0.242}$ is shown in Table 4.1.

Table 4.1 EA result of chitosan starting material (DD 75.8%)

	%C	%H	%N	C/N
Anal. Calcd	45.46	6.71	8.18	5.47
Found	35.2	6.54	6.43	5.56

Generally, chitin-chitosan cannot avoid the trace amount of mineral, especially $CaCO_3$, even from the purification process. Chitosan cannot be decomposed completely without oxidative agent, such as P_2O_5. The EA result is always somewhat different from the calculated data. Thus, C/N ratio was chosen to evaluate the component and the ratio was close to that of the

calculated one. Referring to EA result, the degree of deacetylation should be 74.57% (Scheme 4.1).

Scheme 4.1 Real structure of chitosan starting material

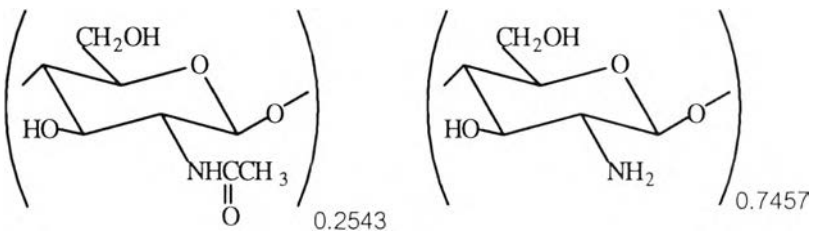

TGA shows the broad peak from 56.27°C to 100°C and the sharp peak at 308.67°C (Figure 4.2). The former peak revealed the loss of moisture content while the latter peak showed the degradation of chitosan.

4.1.2 Microstructure Analysis

Takai *et al.* (1988) reported that crab shell gives a orthorhombic α-chitin with major peak around 19° and minor peaks at 9° and 20°. X-ray diffraction pattern of shrimp shell chitosan are summarized in Figure 4.3.

The XRD pattern of the starting chitosan DD 74.57% shows the crystallinity peaks at 9.44° and 19.9°. This implied that the shrimp shell has the similar α packing structure as the crab shell. After mechanical grinding force, chitosan became less crystallinity structure as can be seen from the broad peak from 5°-30° (Figure 4.3 (c)).

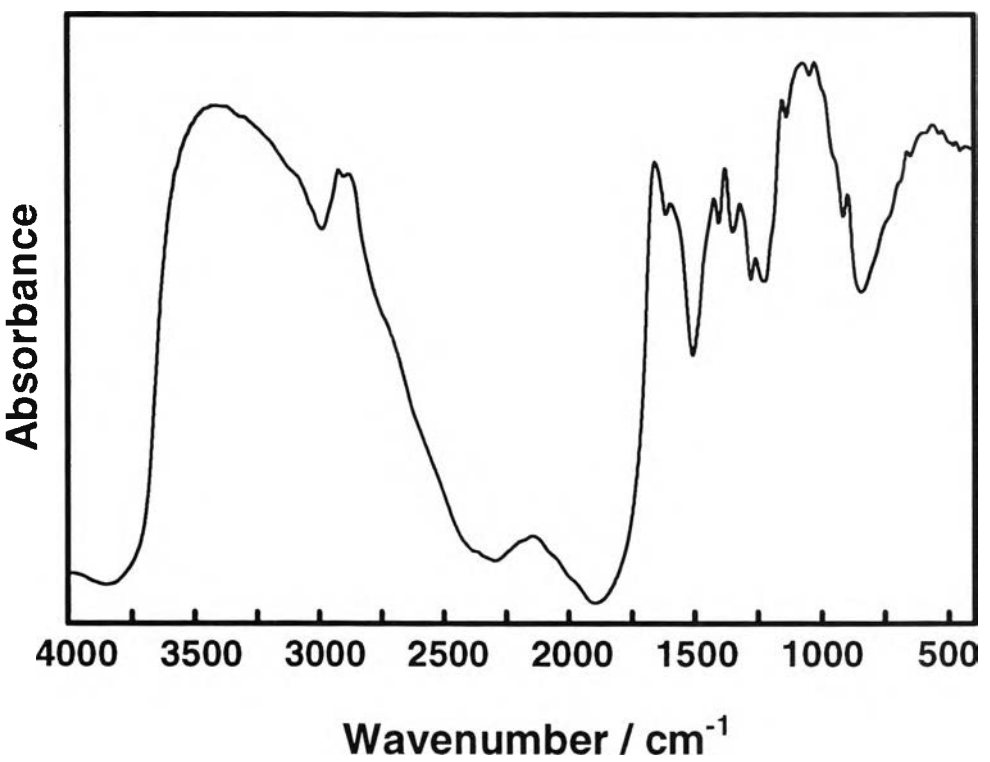

Figure 4.1 FT-IR spectrum of chitosan (DD = 75.8%).
FT-IR (KBr, cm^{-1}):- 3419 (O-H), 2881 (C-H), 1658 (C=O amide), 1596 (NH_2 amine), 1075 (pyranose rings).

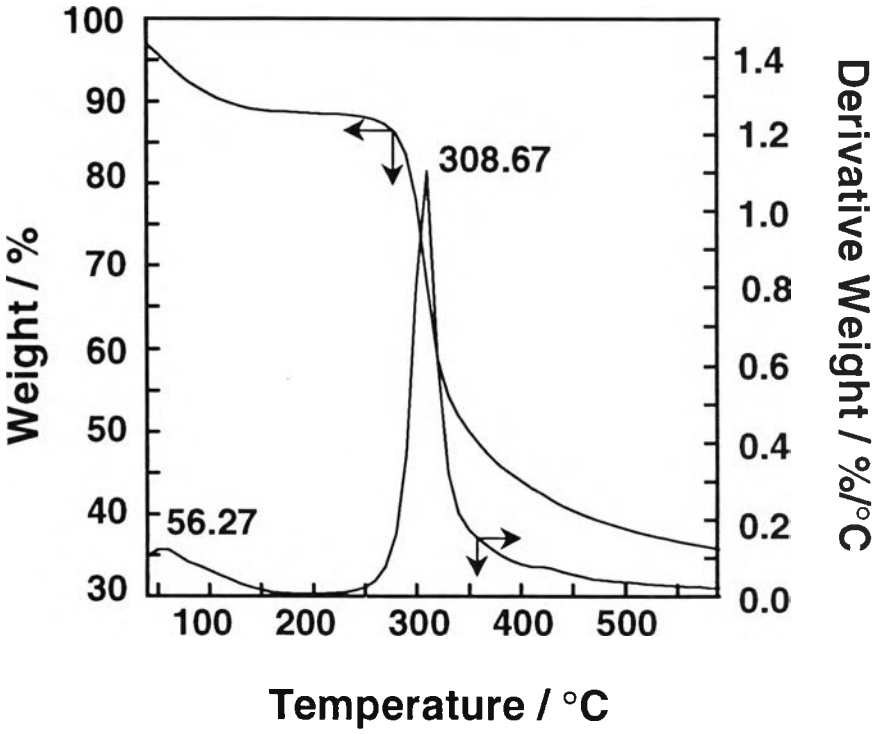

Figure 4.2 TGA diagram of chitosan (DD 74.57%).

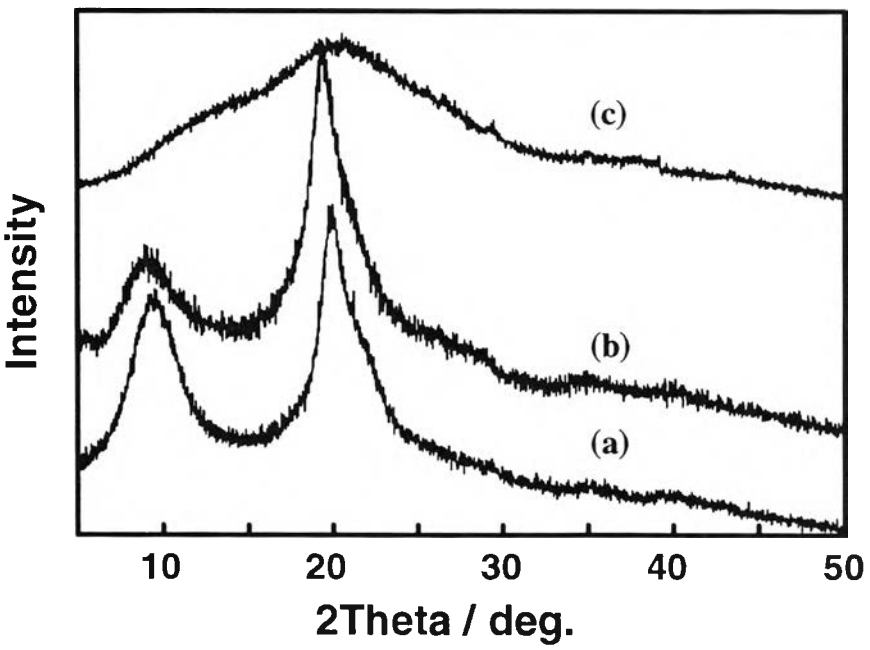

Figure 4.3 XRD patterns of chitosan DD 74.57% (a) starting material; small flake, (b) after cutting with stainless blade; fine flake, and (c) after ball mill 72 h; fine powder.

4.2 Preparation of Chitinase Enzyme

The production chitinase from *Staphylococcus species* strain TU005 (E) depends on variables, such as aeration, cultivation temperature, bacteria growth, and the type of media used for cultivation. In the present work, these variables were fixed to simplify the studies as mentioned in experimental part. Colloidal chitin is an effective source for induction of chitinase production owing to the ease of digestion as compared to the flake chitin (Kuakarun *et al.*, 1998). Colloidal chitin was prepared and added to the culture medium for the *Staphylococcus sp.* to induce the chitinase. The highest activity of enzyme was achieved at 1.5-2 days of cultivation (Figure 4.4), after 2 days the enzyme activity decreased. This may due to depletion of nutrition, death of bacteria or degradation of the enzyme by some proteinases.

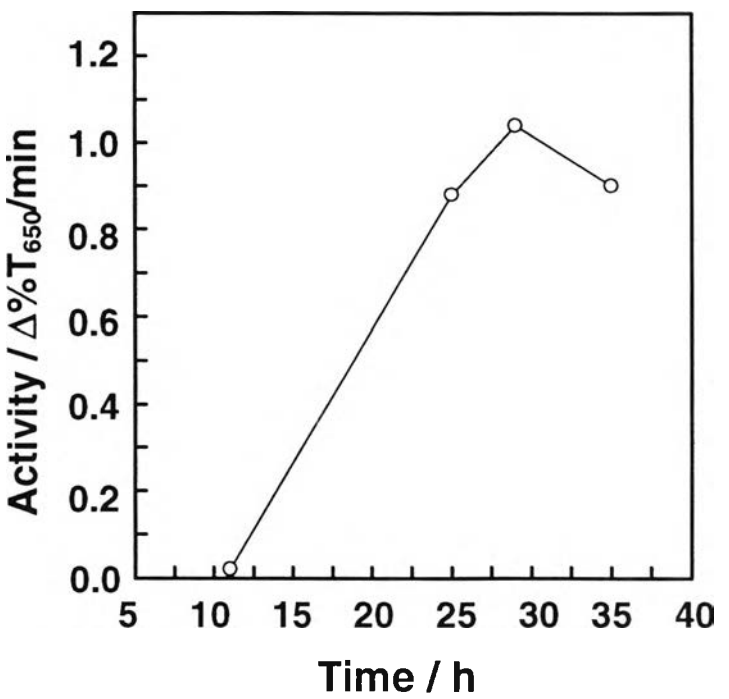

Figure 4.4 Induction of chitinase production in *Staphylococcus species* strain TU005 (E) when grown in colloidal chitin minimum media.

Partial purification by precipitation with $(NH_4)_2SO_4$, is the practical way to exclude other proteins. In our experiments, 80% $(NH_4)_2SO_4$ caused a lost in enzymatic activity of 50% from the crude enzyme preparation, therefore, the enzyme was partially purified by dialysis and then concentrated by using polyethylene glycol (PEG) to remove water and small molecules. After the enzyme was concentrated by PEG for 3 h, the measured activity was 80-90% of its original activity. The enzyme was then prepared into powder form by lyophilization. It was found that the percent yield decreased 35%, from lyophilization process, as determined by turbidimetric assay (Table 4.2).

Chitinases production from different source gives different activity. The activity of chitinase purified from *Streptomyces orientalis* was 4.41 U/mg (Tominaga *et al.*, 1976) while specific activity of purified chitinase from *Vibrio sp.*, was 110 U/mg (Ohtakara *et al.*, 1979). The activity of chitinase can also be assayed by a colorimetric assay, measuring reducing sugar during the enzymatic degradation process. The amount of reducing sugar produced can be determined using standard N-acetylglucosamine solution to generate a standard calibration curve. The colorimetric analysis showed that purified enzyme has an activity of 18 mU/mg.

Table 4.2 Activity of enzyme obtained from each preparation step

Preparation step	Turbidimetric assay			
	Total volume (mL or mg)	Activity ($\Delta\%T_{650}$/min/mL)	Total activity ($\Delta\%T_{650}$/min)	% yield
Crude enzyme	275.75 ± 140.33	0.952 ± 0.34	190.29 ± 115.34	100
PEG absorbed enzyme	53.375 ± 10.125	2.95 ± 1.5	167.32 ± 104.93	87.64 ± 9.85
Lyophilized enzyme	362.575 ± 336.78	0.35 ± 0.17 [a]	86.6 ± 22.28	35.130 ± 1.67

[a] $\Delta\%T_{650}$/min.mg.

4.3 Factors Effecting Enzyme Hydrolysis on Chitosan Chain

The factors effecting enzyme digestion were studied, i.e., hydrolysis time, amount of substrate, and amount of enzyme used in a reaction.

4.3.1 Effect of Hydrolysis Time

The enzyme denatures with time, in a reaction. The enzyme stability determines the period time in which an enzyme can function in a reaction. As shown in Figure 4.5, in either 0.1 M phosphate buffer or 0.2 M acetate buffer, chitinase activity decreases gradually to 50% of its initial activity after 2 h. There were only 10% of the activity left after 3-4 h. This suggests that the incubation time for our reactions should be within 2 h.

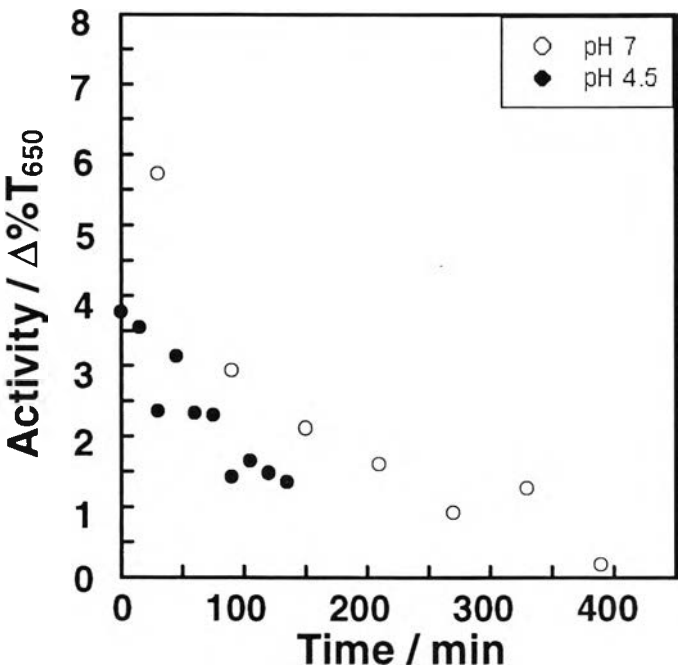

Figure 4.5 Enzyme stability in: ○ phosphate buffer (0.1 M) pH 7; and ● acetate buffer (0.2 M) pH 4.5.

4.3.2 Effect of Substrate Concentration

The solvent for dissolving chitosan should be considered according to the nature of chitosan and enzyme used. Acetic acid is one of the best solvents for chitosan, while enzyme functions at neutral or weak base/acid condition.

However, if the pH of the reaction mixture is too low, the enzyme could not function well. The viscosity and substrate concentration also effects the way an enzyme works. Higher viscosity of the solution will decrease rate of enzymatic reaction. Therefore, the enzyme activity was studied in various chitosan acetic solutions. The stability of the enzyme in these reactions was also studied.

Figure 4.6 shows that at 2% chitosan concentration (d), the decrease in viscosity of chitosan was not as high at that of higher concentration (a, b, and c).

Figure 4.7 shows the enzymatic degradation rate. It was found that at 4% concentration (a), the degradation proceeded at 0.81 cP/min, which are the highest degradation rate observed in this experiment. However, chitosan solution was nearly saturated at this concentration. At lower concentration (d), the degradation rate proceeded very slowly.

At low substrate concentration, the probability of enzyme-substrate formation is low. The enzymatic degradation at saturated concentration (4%) was the optimum condition in out set of experiment.

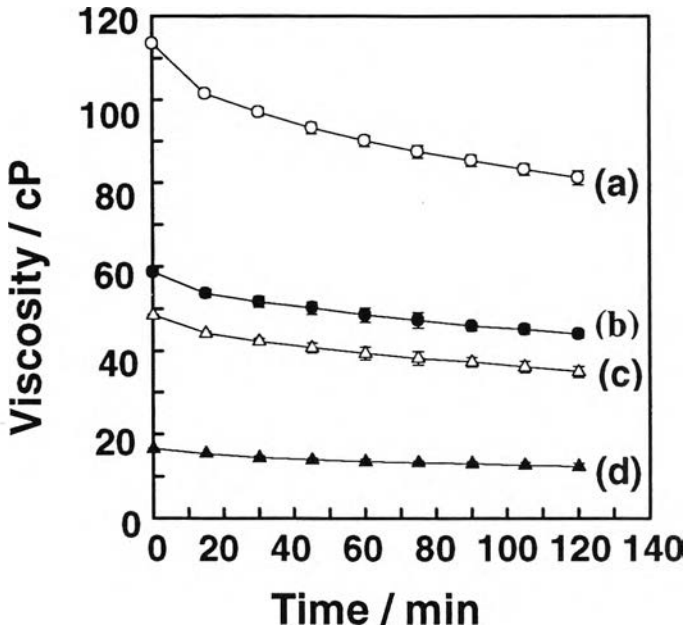

Figure 4.6 Viscosity reduction of chitosan solution when treated with chitinase 18 mU/mL of chitinase was used to digest (a) 4% chitosan, (b) 3.5% chitosan, (c) 3% chitosan, and (d) 2% chitosan, at 37°C.

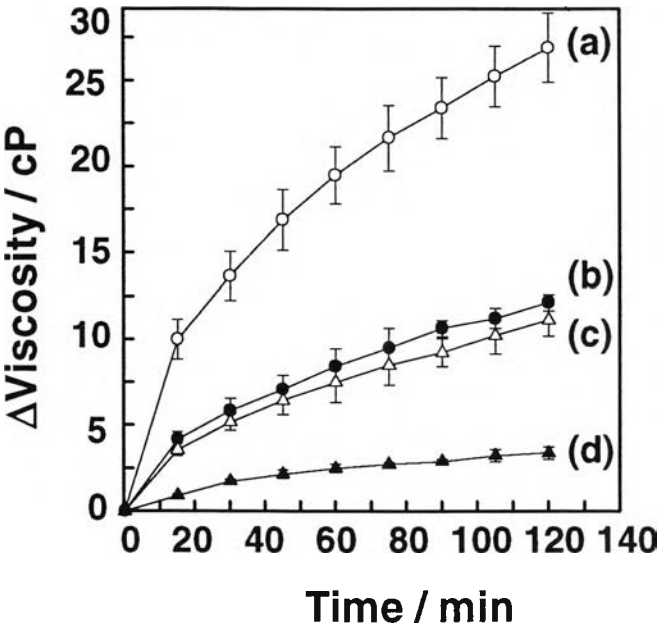

Figure 4.7 Enzymatic degradation rate of chitosan using chitinase 18 mU/mL at 37°C of (a) 4% chitosan, (b) 3.5% chitosan, (c) 3% chitosan, and (d) 2% chitosan.

4.3.3 Effect of Enzyme Concentration

The minimum amount of enzyme to obtain the highest rate of chitosan degradation was studied by fixing the amount of substrate and varying the amount of enzyme used in the reaction. The amount of enzyme was varied from 4.5 mU/mL to 30 mU/mL, as shown in Figure 4.8. The rate of viscosity reduction at initial phase was significant. The amount of enzyme 9 mU/mL gave the rate of 0.48 cP/min, which was close to the reaction rate when, 18 and 30 mU/mL of enzyme was used. This suggested that the minimum amount of enzyme for the degradation should be the range of 9-18 mU/mL. However, the enzyme half-life in the reaction was found to exceed the period of 2 h previously observed (Figure 4.5). It also should be noted that the viscosity of chitosan solution continues to decrease over 4 h. This indicates that the enzyme was stable for longer periods of time in the reaction mixture containing chitosan.

In conclusion, the optimum degradation condition was 4% chitosan concentration with 18 mU/mL of chitinase.

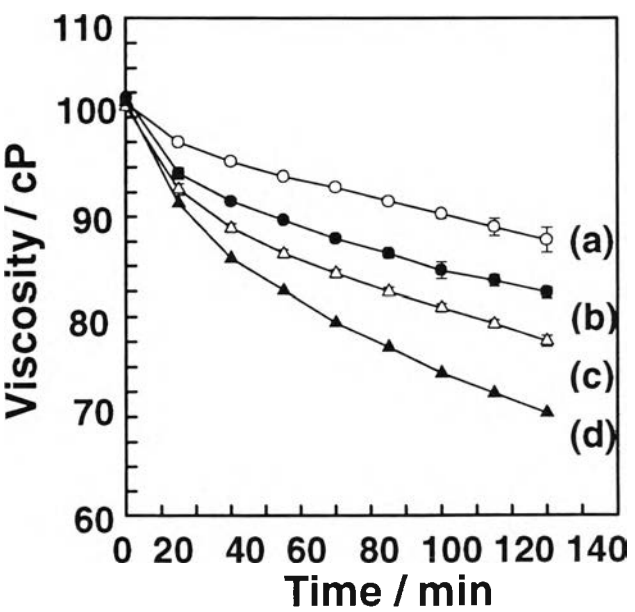

Figure 4.8 Enzymatic degradation of 4% chitosan with chitinase at 37°C with enzyme amount of (a) 4.5 mU/mL, (b) 9 mU/mL, (c) 18 mU/mL, and (d) 30 mU/mL.

4.4 Characterization of Oligochitosan

4.4.1 Molecular Weight

After the treatment with enzyme, the viscosity decreased gradually when the enzyme was added for 4 times, i.e., after enzyme treatment 1, 2, 3, and 4 days (Figure 4.9). The viscosity decreased rapidly to 45% of the initial viscosity of chitosan starting material when the enzyme was added at the first time. This indicated that the large amount of chitin unit was degraded from chitosan chain. The viscosity decreasing of chitosan chain was dependent on the amount of chitin unit and the ability of enzyme. Even though much amount of enzyme was added, the viscosity did not change significantly. This reflected that the starting material contained a limit amount of chitin and after degradation at chitin unit the reaction terminated.

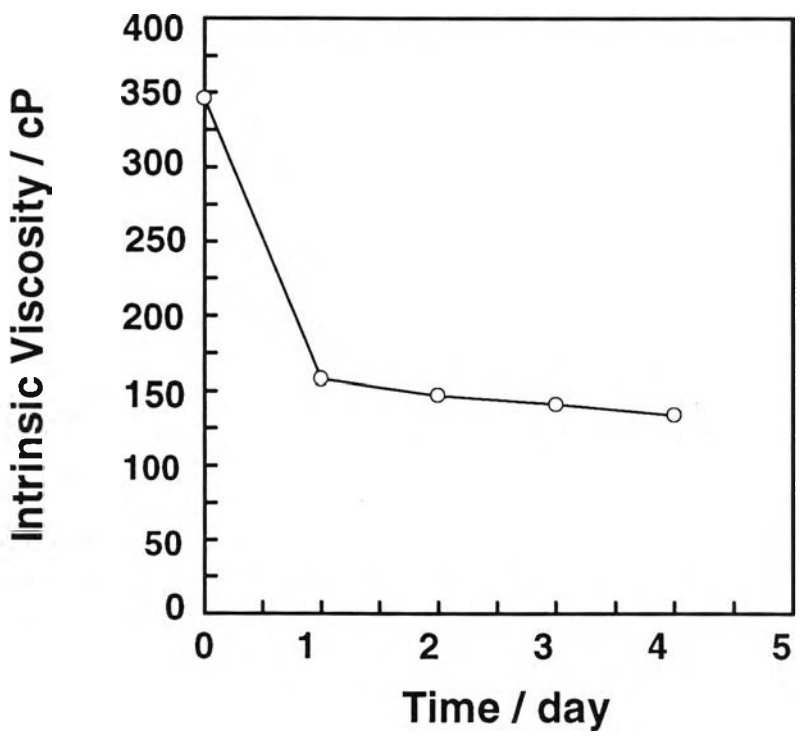

Figure 4.9 Intrinsic viscosity of chitosan after treatment enzyme for several days when enzyme was added for 18 mU/mL in 1, 2, 3, and 4 days.

4.4.2 Chemical Structure of Oligochitosan

FT-IR spectra of the oligochitosan obtained from various degradation conditions were studied. Figure 4.10 shows that after enzymatic degradation, the characteristic peaks of amide I and II of chitin are decreased at 1655 and 1550 cm^{-1}, respectively. The quantitative FT-IR analysis was used to confirm the decreasing of these peaks by comparing amide I and II peaks to the C-H peak at 2878 cm^{-1} (Sannan *et al.*, 1978). The plot of the ratio of the absorbance of the amide II band at 1550 cm^{-1} to that of the C-H band at 2878 cm^{-1} against the different degradation conditions are shown in Figure 4.11. This demonstrated that the enzymatic degradation with chitinase enzyme removed some chitin unit out of the chitosan chain. As comparing Figure 4.11 to Figure 4.9, it should be noted that the decrease of viscosity was limited at a certain level might relate to the fact that chitin unit removed by chitinase from the polymer chain. As a result, the enzyme treatment more than 1 day showed the viscosity decreased slightly and at the same time only small amount of chitin unit remained in the chitosan oligomer chain.

The elemental analysis (EA) result of oligochitosan is shown below:

Anal. Calcd for $(C_8H_{13}NO_5)_{0.2543}$ $(C_6H_{11}NO_4)_{0.7457}$: %C, 45.49%; %H, 6.70%; %N, 8.15%. Found: %C, 38.87; %H, 7.28; %N, 7.16.

The C/N ratio of calculated data was 5.58 while that of the found data was slightly lower to be 5.43. This may be because the decomposition of chitosan is known to require the oxidative agent such as P_2O_5 to help the complete combustion in elemental analysis instrument.

Figure 4.12 shows TGA diagram of oligochitosan. The initial weight loss at 57.85°C referred to the loss of moisture. The second peak at 303.05°C revealed the degradation temperature of oligochitosan at glycoside bond breaking. By comparing oligochitosan to the chitosan starting material (T_d = 308.67°C), the degradation temperature of oligochitosan was close to that of

chitosan. This implied that the enzymatic degradation had little effect on the thermal property of chitosan.

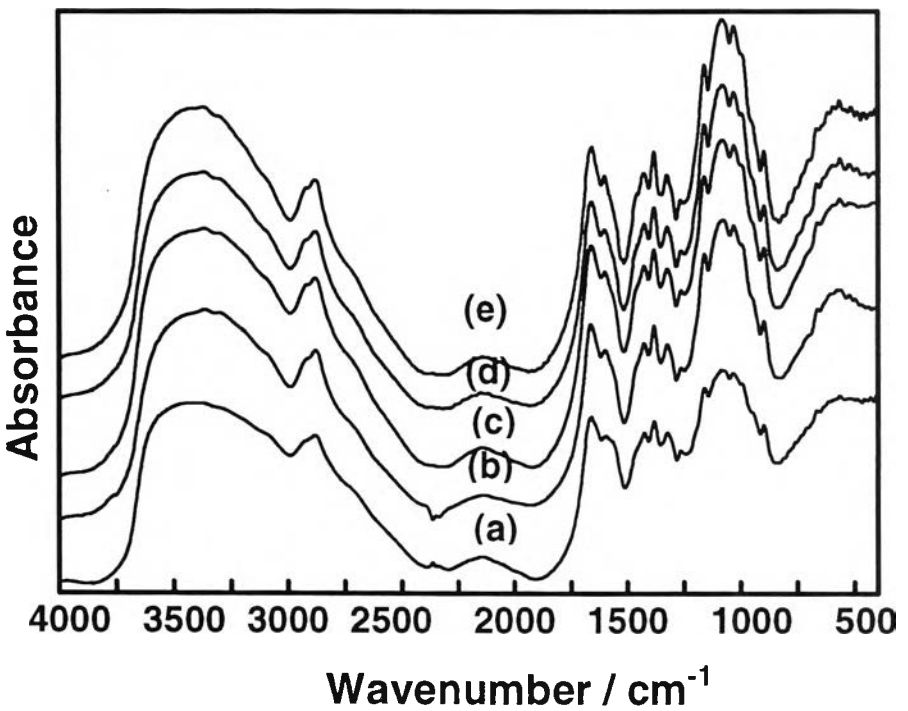

Figure 4.10 FT-IR spectra of oligochitosan in (a) reprecipitated undigested chitosan with 1 M NaOH, (b) reprecipitated of chitosan after enzyme treatment of 18 mU/mL for 1 day, (c) reprecipitated of chitosan from (b) with an addition of 18 mU/mL of enzyme at the end of the first day, (d) reprecipitated of chitosan from (c) with an addition of 18 mU/mL of enzyme at the end of the second day, and (e) reprecipitated of chitosan from (d) with an addition of 18 mU/mL of enzyme at the end of the third day.

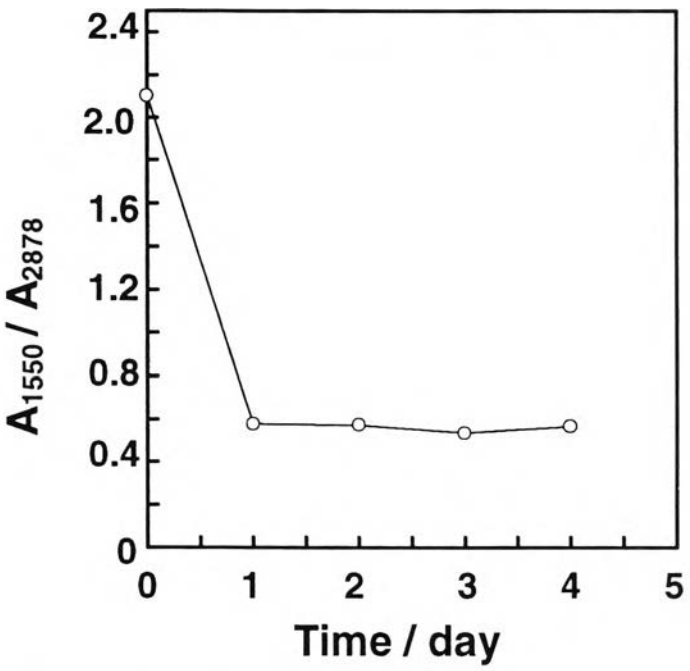

Figure 4.11 Quantitative analysis of oligochitosan comparing the amide II band to C-H band (A_{1550}/A_{2878}) by FT-IR.

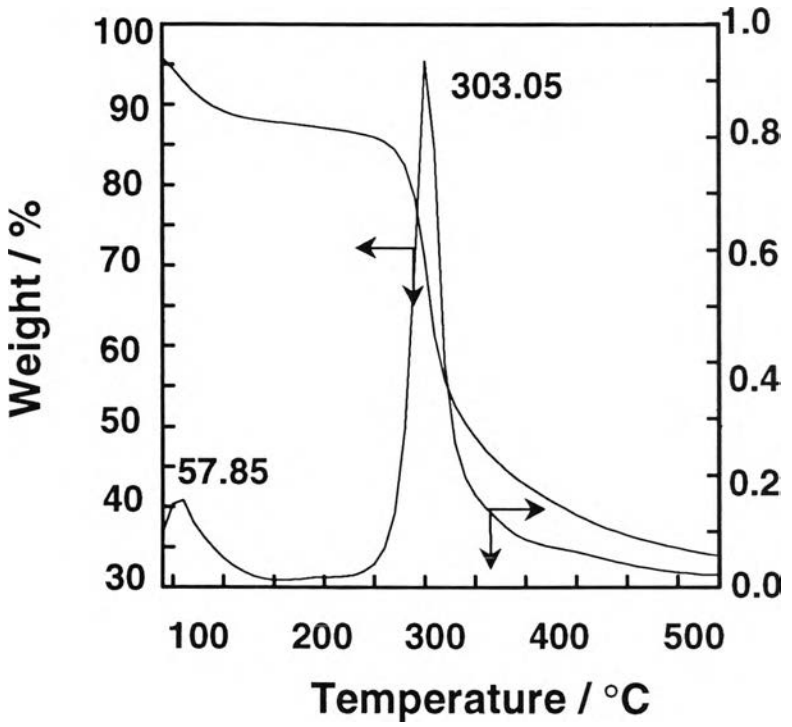

Figure 4.12 TGA diagram of oligochitosan.

4.4.3 Microstructure Study

The enzymatic hydrolysis gave the changing of structure as shown in the X-ray patterns (Figure 4.13). The peaks of chitosan after enzymatic hydrolysis were broad at 10° and 20°, while untreated chitosan showed the sharp peaks. The results implied that the enzymatic treatment induced the amorphous part in microstructure.

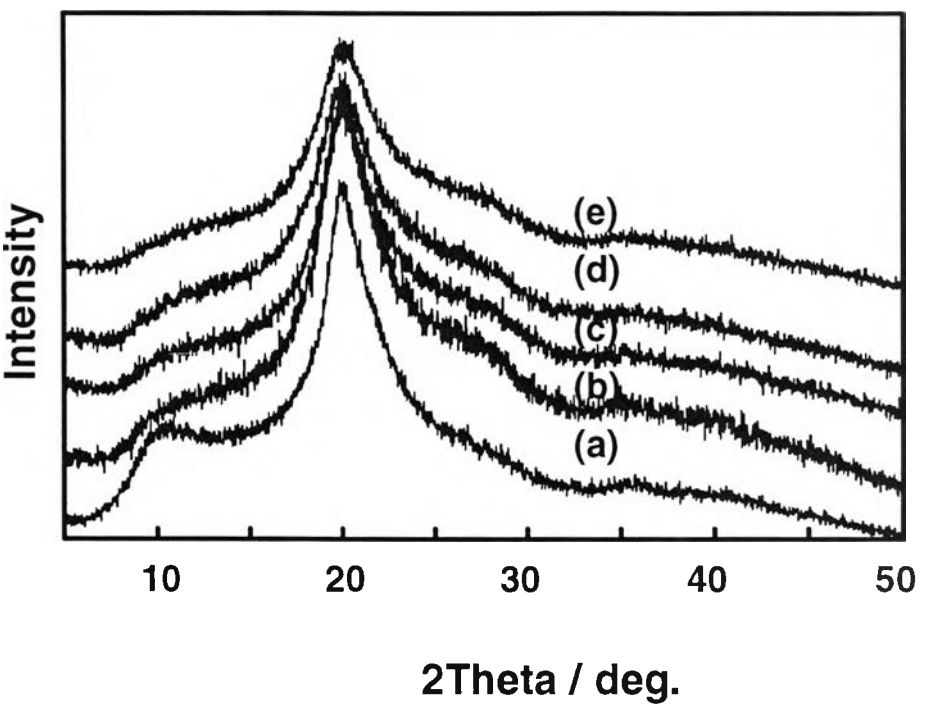

Figure 4.13 XRD patterns of (a) reprecipitated undigested chitosan with 1 M NaOH, (b) reprecipitated of chitosan after enzyme treatment of 18 mU/mL for 1 day, (c) reprecipitated of chitosan from (b) with an addition of 18 mU/mL of enzyme at the end of the first day, (d) reprecipitated of chitosan from (c) with an addition of 18 mU/mL of enzyme at the end of the second day, and (e) reprecipitated of chitosan from (d) with an addition of 18 mU/mL of enzyme at the end of the third day.

4.5 Preparation of Oligochitosan Derivatives

In the previous part, it was confirmed that the structure of chitosan after enzymatic degradation was maintained. Here, the chemical modification of oligochitosan was studied under the same approach for chitosan. In general, chitosan unit can be modified at C-6 hydroxyl group and C-2 amino group. In the present work, oligochitosan was modified to a reactive precursor by focusing on chemical modifications at the C-6 position.

4.5.1 Preparation of N-phthaloyloligochitosan

Oligochitosan, as same as chitosan, has three reactive group, i.e., amino, primary alcohol, and secondary alcohol groups. In order to simplify the reaction, we concentrated on OH at C-6, protecting group at amino group. Ideally, the protecting group should be attached in the chain efficiently and be resistant to acidic or basic hydrolysis, and oxidation. There are many protecting groups such as sulfonamide, phenacyl group, phthaloyl group, etc (Hendrickson *et al.*, 1970). N-phthaloylation is concerned to be a useful pathway to protect amino group of chitosan, especially, in order to focus the reaction at C-6 hydroxyl group. The phthaloyl group also can be removed easily by treatment with hydrazine hydrate at 100°C (Nishimura *et al.*, 1991). As shown in Figure 4.14, the FT-IR spectra show characteristic absorptions due to phthalimido groups at 1775 and 1714 cm^{-1}.

The elemental analysis (EA) result of N-phthaloyloligochitosan;

Anal. Calcd for $(C_8H_{13}NO_5)_{0.2543}(C_{14}H_{13}NO_6)_{0.6991}$:- %C, 55.3; %H, 4.92; %N, 5.33. Found: %C, 46.46; %H, 5.96; %N, 5.01.

The calculation of elemental analysis showed that the phthalic anhydride was not reacted with NH_2 group completely. The result implied that the phthalic anhydride was introduced for 93.75% as shown in Scheme 4.2.

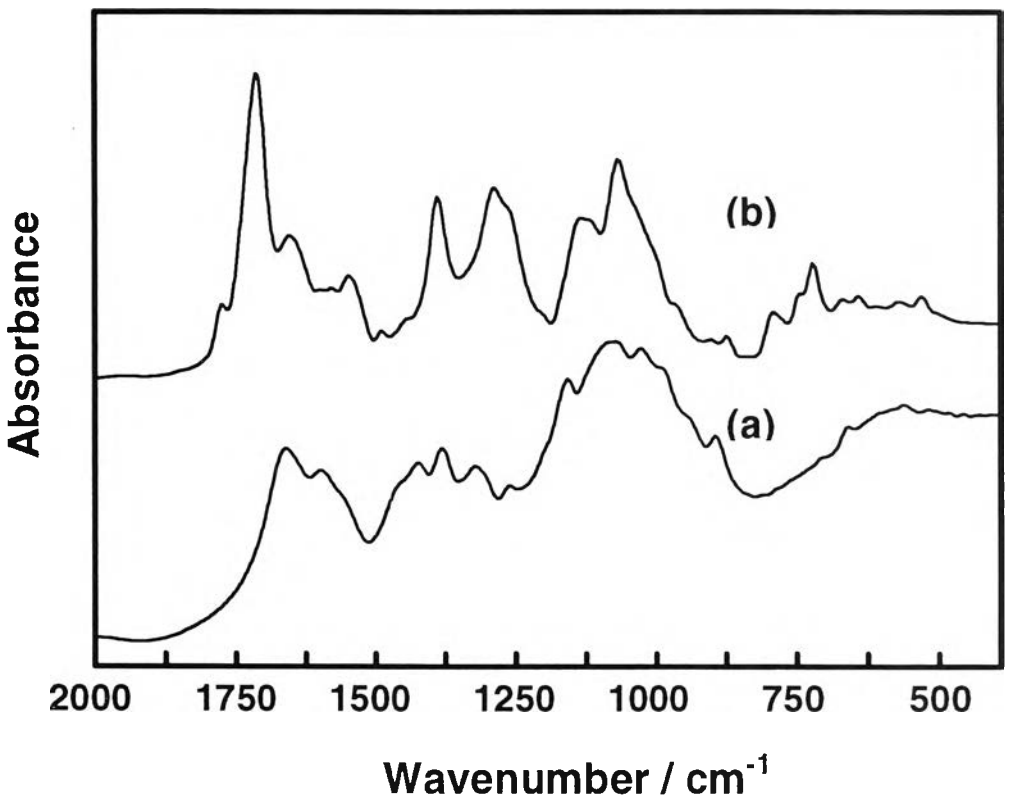

Figure 4.14 FT-IR spectra of (a) oligochitosan, and (b) N-phthaloyloligochitosan.

Scheme 4.2 Structures of phthaloyloligochitosan with the degree of deacetylation 74% (a) ideal structure for completion of phthaloyl group, and (b) 93% phthaloyl formation structure

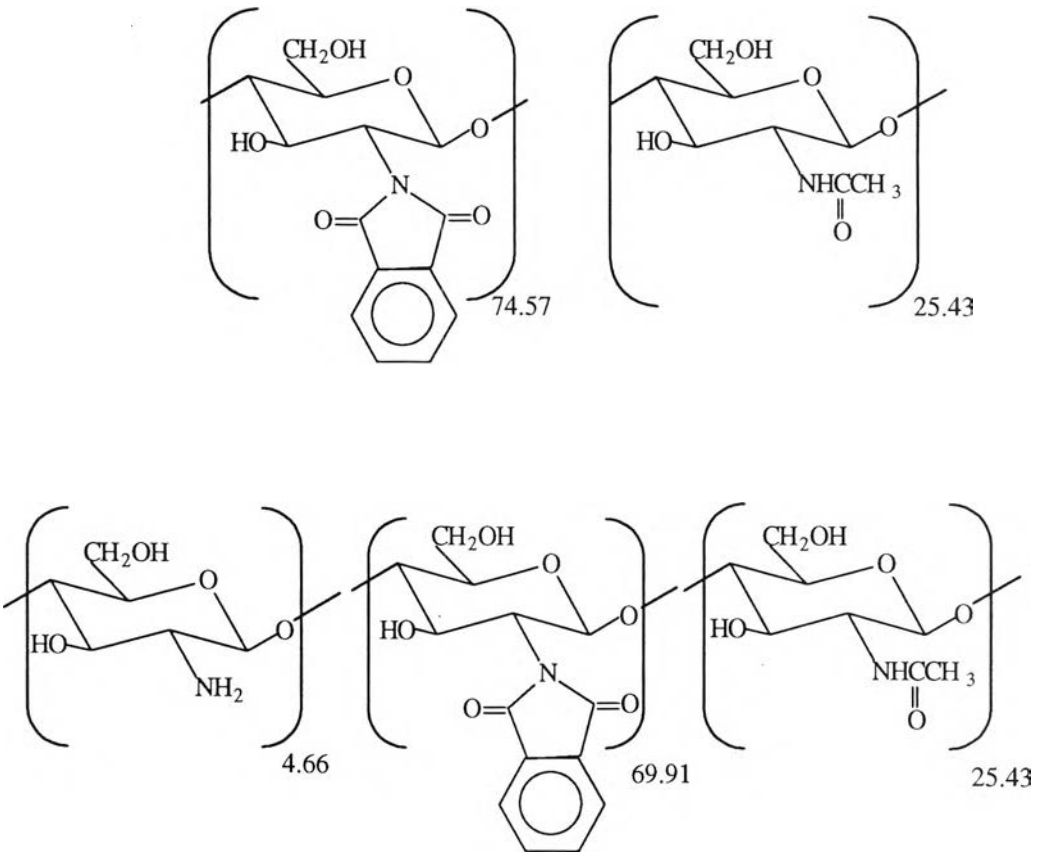

TGA diagram of phthaloyloligochitosan is shown in Figure 4.15. The initial weight loss until 100°C referred to the loss of moisture and the following peak at 213.61°C revealed the loss for phthalimido group. The latter peak at 360.73°C reflected the breaking of glycoside linkages. The degradation temperature of modified chitosan was 57.68°C higher than that of the unmodified chitosan. Unexpectedly, the introduction of phthaloyl group onto chitosan, even it was a bulky group, the thermal stability was improved. This may due to the more rigid packing structure of phthaloyloligochitosan, which may come from ionic interaction of carbonyl group and phenyl ring stacking conformation.

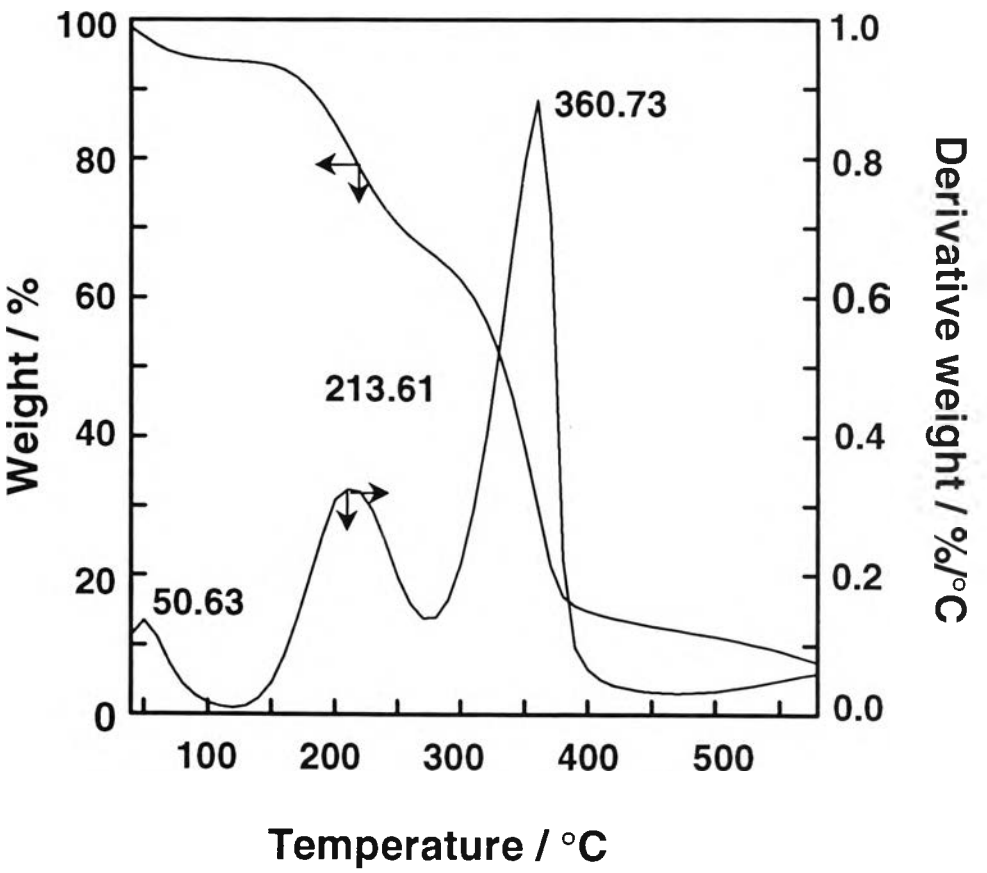

Figure 4.15 TGA diagram of N-phthaloyloligochitosan.

^{1}H-NMR spectrum of phthaloyloligochitosan showed proton peaks due to acetyl methyls at 2.5 ppm, pyranose rings at 3-5.5 ppm, aromatic rings of phthalimido groups at 7-8 ppm (Figure 4.16). This implied the successful in phthaloylation on oligochitosan.

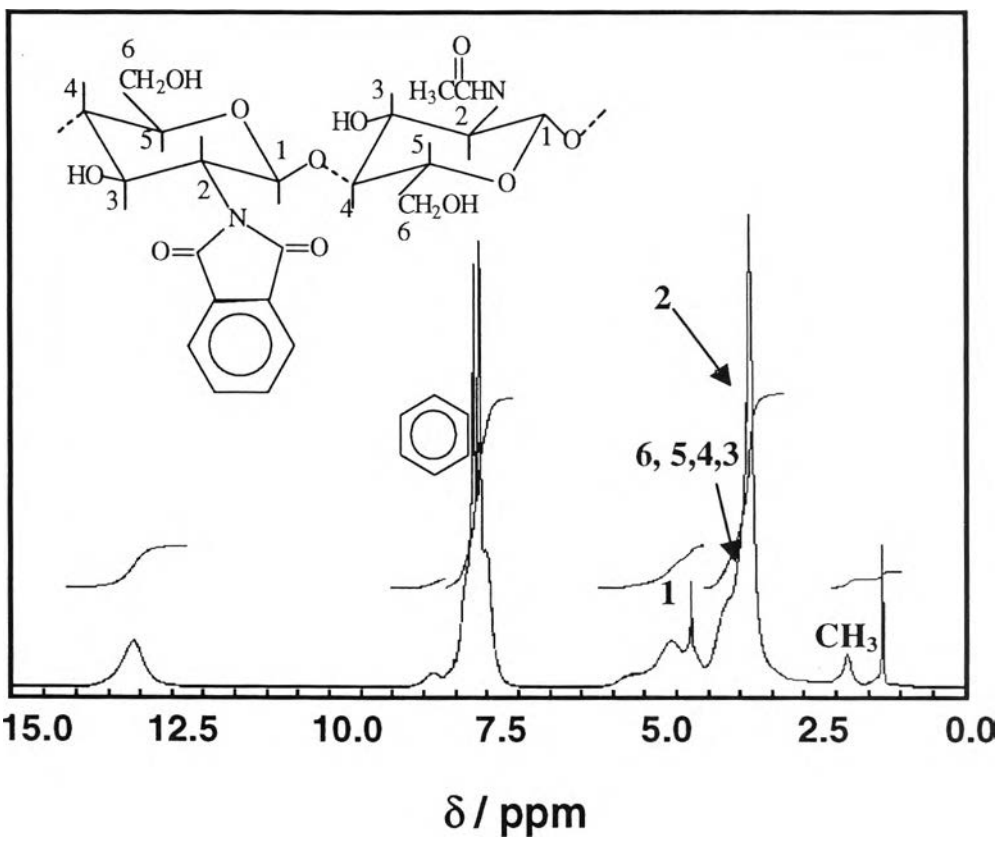

Figure 4.16 ^{1}H-NMR spectrum of N-phthaloyloligochitosan.

UV spectra showed the characteristic peak of phthaloyl group at 237 nm released by 1 M NaOH as comparing to the pure phthalic anhydride. This result confirmed the success of phthaloylation of oligochitosan (Figure 4.17).

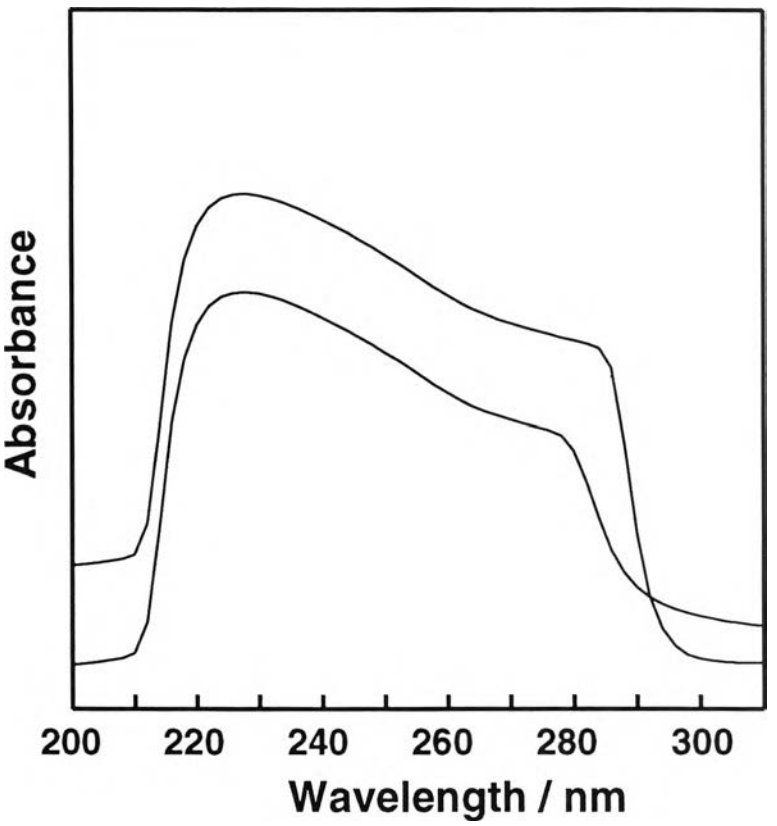

Figure 4.17 UV spectra of (a) pure phthalic anhydride, and (b) N-phthaloyloligochitosan.

4.5.2 Preparation of O-tosyl-N-phthaloyloligochitosan

Tosyl group is one of the most effective leaving groups widely used in carbohydrate chemistry. Moreover, the tosyl group provides more solubility and shows high reactivity under mild condition (Kurita *et al.*, 1992). The tosylation of chitosan is considered to be a versatile precursor for the novel derivatives. O-tosyl-N-phthaloyloligochitosan was prepared using the same procedure as O-tosyl-N-phthaloylchitosan (Nishimura *et al.*, 1991). The reaction was operated in pyridine at room temperature under homogeneous system.

Figure 4.18 shows a characteristic peak at 1173 cm^{-1} attributed to tosyl groups and at 1599 and 817 cm^{-1} due to *p*-phenylene groups. This implied that the tosylation was successful.

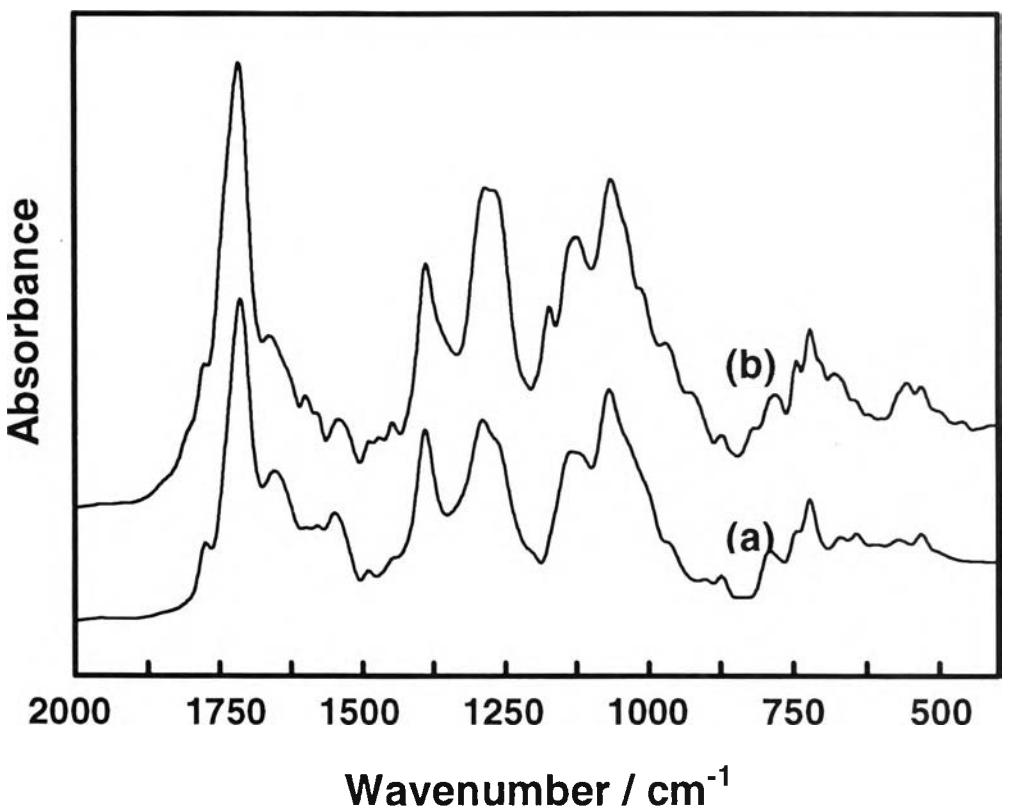

Figure 4.18 FT-IR spectra of (a) N-phthaloyoligochitosan, and (b) O-tosyl-N-phthaloyloligochitosan.

The elemental analysis (EA) result of O-tosyl-N-phthaloyloligochitosan as follows; Anal. Calcd for $(C_{15}H_{19}NSO_7)_{0.2543}(C_{21}H_{19}NSO_8)_{0.6991}(C_{20}H_{23}NS_2O_8)_{0.0466}$: %C, 55.02; %H, 4.53; %N, 7.9; %S, 7.9. Found: %C, 55.67; %H, 4.73; %N, 3.58; %S, 2.37.

Elemental analysis revealed the significant sulfur content. The found S/N ratio was equal to 0.66 while the calculation from the ideal structure was about 2.39 (Scheme 4.3). This implied that the substitution occurred about 27.62% at both hydroxyl group and amino group on the chitosan chain.

Scheme 4.3 Ideal structure of tosylation of phthaloyloligochitosan when the reaction is completed to make the S/N ratio be 2.39

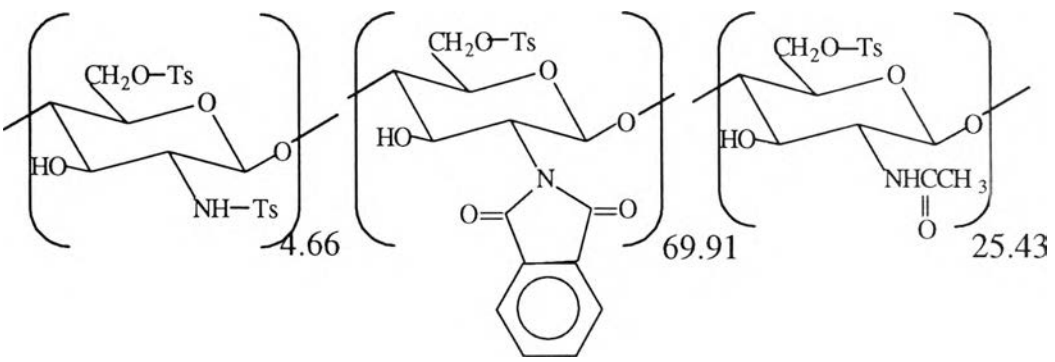

TGA diagram of O-tosyl-N-phthaloyloligochitosan (Figure 4.19) indicates the significant weight loss at 229.34°C due to the loss of tosyl group. The minor peak at 347.61°C revealed the glycoside linkage breaking.

UV spectra show the peak at 361 nm (Figure 4.20) which can be referred to aromatic group. This result confirmed the successful in O-tosyl-N-phthaloyloligochitosan.

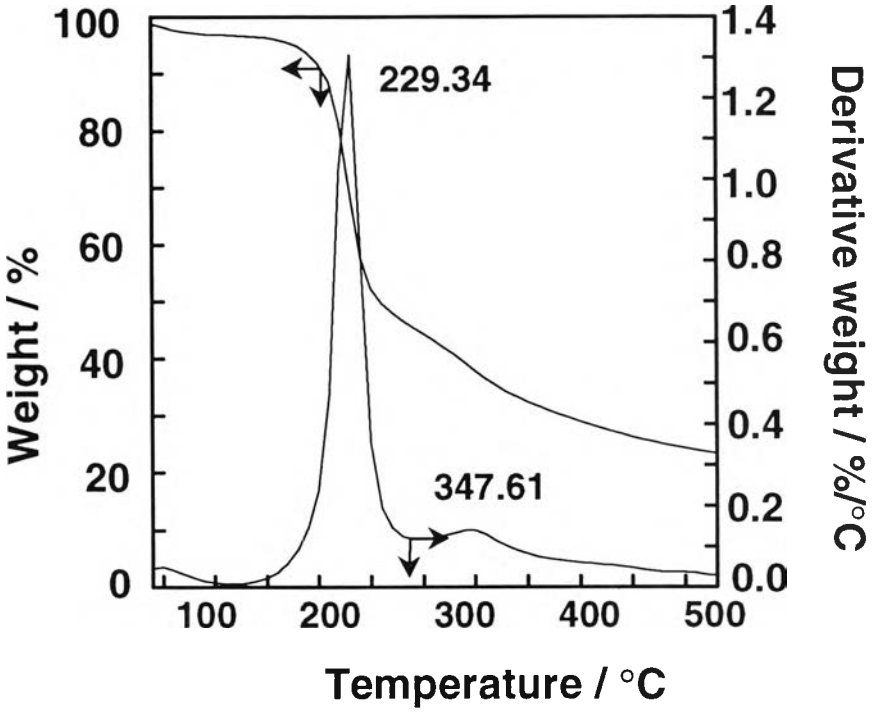

Figure 4.19 TGA diagram of O-tosyl-N-phthaloyloligochitosan.

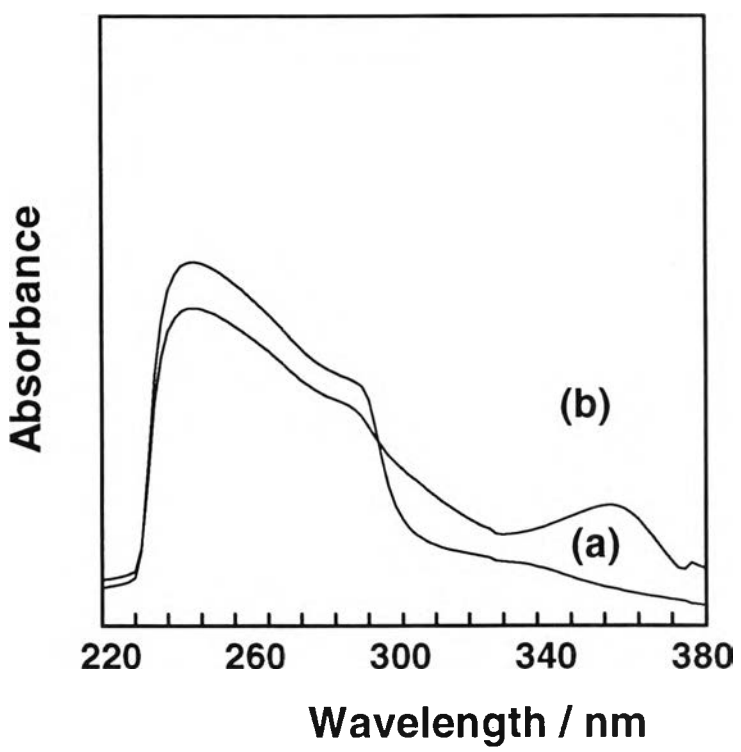

Figure 4.20 UV spectra of (a) N-phthaloyloligochitosan,

and O-tosyl-N-phthaloylchitosan.

4.5.3 Preparation of O-lauryl-N-phthaloyloligochitosan

Hexanoyl, decanoyl, and dodecanoylchitin were prepared by using acyl chlorides in methanesulfonic acid (Kaifu *et al.*, 1981). Ideally, chitosan has to be completely dissolved in organic solvent in order to have the homogeneous reaction proceeded effectively. In the present work, O-tosyl-N-phthaloyloligochitosan was tested for various organic solvents to find that it was well dissolved in pyridine. The reaction between lauric acid and O-tosyl-N-phthaloyloligochitosan was performed in homogeneous system to enhance the efficiency of the reaction.

The FT-IR spectroscopy was applied to clarify the coupling of long chain alkyl by observing methylene group. Figure 4.21 shows the peaks at 2926, 1460, 726 for the lauryl group.

The elemental analysis of O-lauryl-N-phthaloyloligochitosan is as follows,

Anal Calcd for $(C_{20}H_{35}NO_6)_{0.2543}(C_{26}H_{35}NO_7)_{0.6991}(C_{18}H_{33}NO_5)_{0.0466}$: %C, 65.06; %H, 7.85; %N, 3.15. Found: %C, 55.59; %H, 4.58; %N, 3.38.

The ideal structure of O-lauryl-N-phthaloyloligochitosan (Scheme 4.4) shows the C/N ratio is about 20.65 while it was found for 16.45. This result implied that the lauryl group substitution was achieved for 79.66%.

Scheme 4.4 Ideal structure of laurylation of tosylphthaloyloligochitosan when the reaction is completed

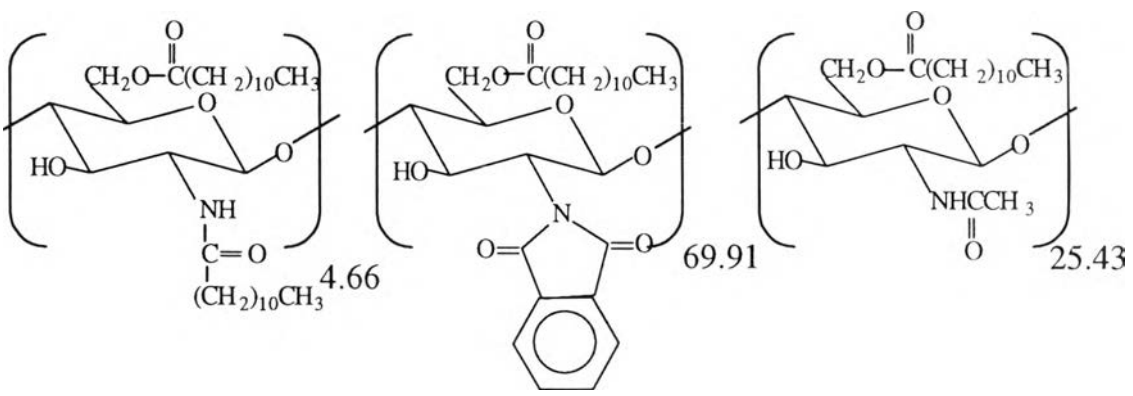

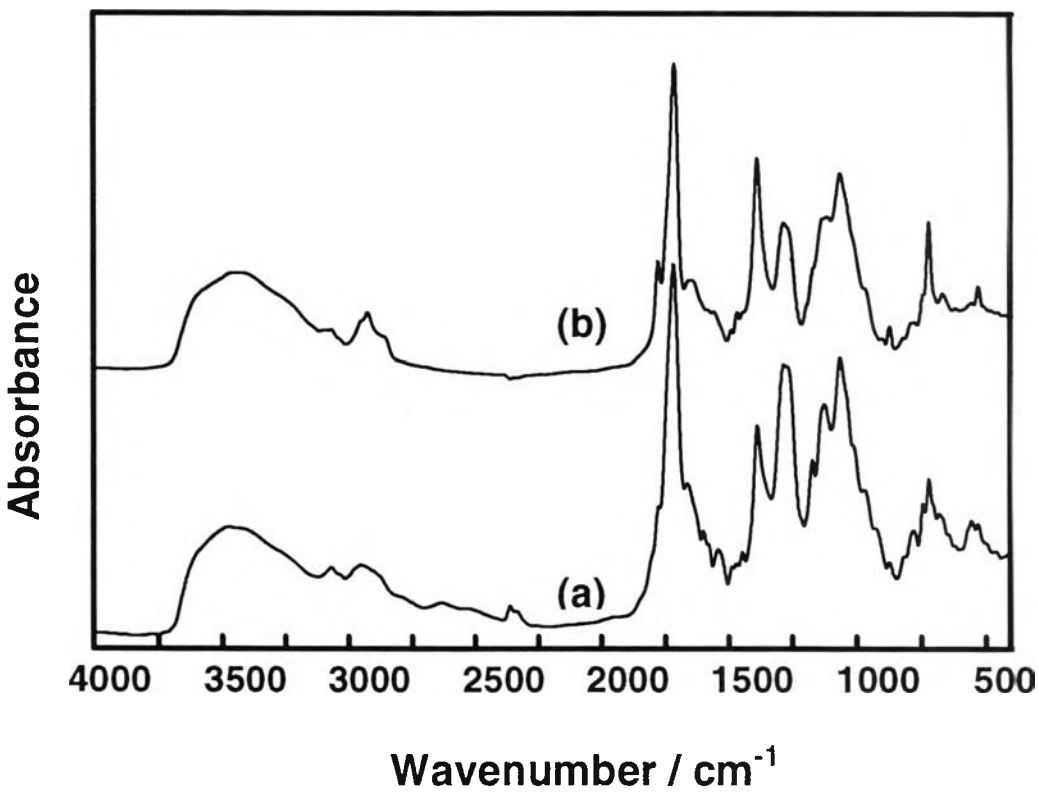

Figure 4.21 FT-IR spectra of (a) O-tosyl-N-phthaloyloligochitosan, and (b) O-lauryl-N-phthaloyloligochitosan.

TGA diagram of O-lauryl-N-phthaloyloligochitosan showed the weight loss at 288°C, which was decreased for 15°C from the oligochitosan (Figure 4.22). This might reflect from the fact that laurylation caused a decrease of thermal stability due to the interaction of long chain. The introduced lauryl group decreased the chain packing and the thermal stability.

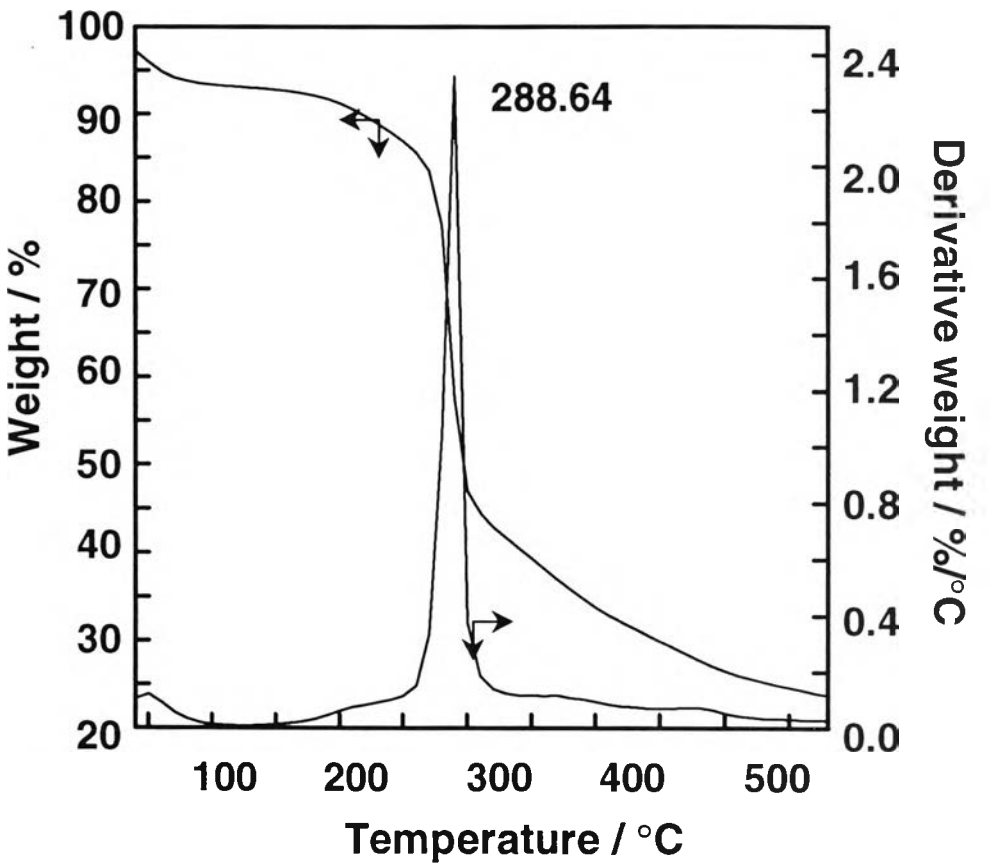

Figure 4.22 TGA diagram of O-lauryl-N-phthaloyloligochitosan.

The successful preparation of O-lauryl-N-phthaloyloligochitosan was also confirmed by the tosyl peak at 361nm (Figure 4.23) which was decreased after the derivatives obtained.

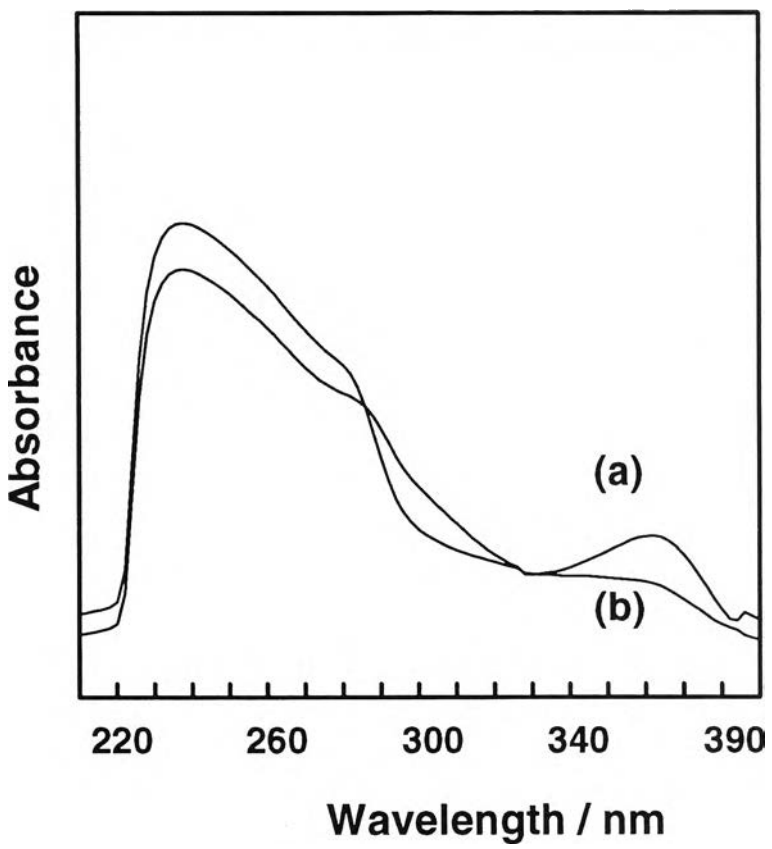

Figure 4.23 UV spectra of (a) O-tosyl-N-phthaloyloligochitosan, and (b) O-lauryl-N-phthaloyloligochitosan.

4.6 Microstructure Study of Oligochitosan Derivatives

It is interesting to study how the changing in the chemical structure effects the molecular packing structure. The XRD patterns of N-phthaloyloligochitosan, O-tosyl-N-phthaloyloligochitosan, and O-lauryl-N-phthaloyloligochitosan are shown in Figure 4.24. The XRD pattern of N-phthaloyloligochitosan shows the amorphous region from 10° to 30°. By introducing the bulky group on the chitosan main chain, the inter- and/or intra-hydrogen bonding of amino and/or acetamide group among the neighbor chain were eliminated. O-tosylation and O-laurylation showed the less crystallinity

than N-phthaloyloligochitosan as confirmed from the broader peaks at 2θ of 10°, and 20°.

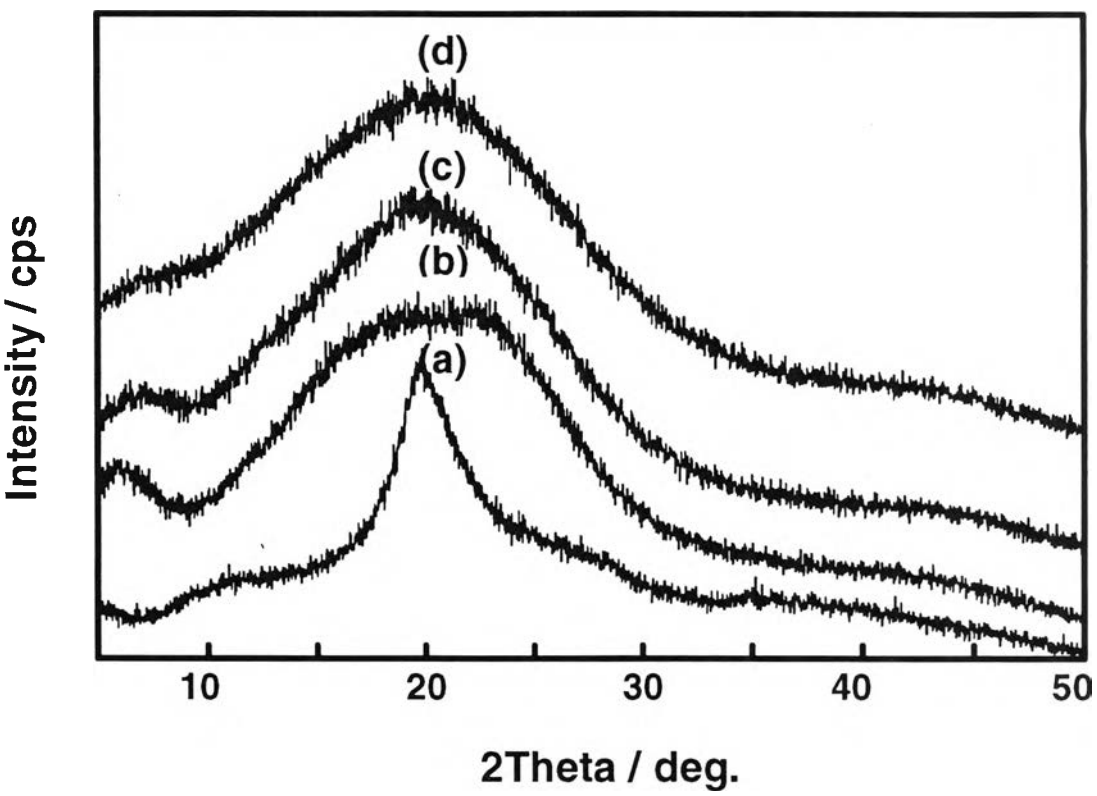

Figure 4.24 XRD patterns of (a) oligochitosan, (b) N-phthaloyl oligochitosan, (c) O-tosyl-N-phthaloyloligochitosan, and (d) O-lauryl-N-phthalic anhydride.